

Brain Tumor Segmentation in the Sub-Saharan African Population Using Segmentation-Aware Data Augmentation and Model Ensembling

Claudia Takyi Ankomah¹[0009-0004-7139-6927], Livingstone Eli Ayivor¹, Ireneaus Nyame², Leslie Wambo¹, Patrick Yeboah Bonsu³, Aondona Moses Iorumbur⁵, Raymond Confidence⁵, and Toufiq Musah¹

¹ Kwame Nkrumah University of Science and Technology, Kumasi, Ghana.

² University of Cape Coast, Cape Coast, Ghana.

³ University of Toronto, Toronto, Canada

⁴ Department of Biomedical Engineering, McGill University, Montreal, Canada.

⁵ Department of Physics, Federal University of Technology, Minna, Nigeria.

Abstract. Brain tumors, particularly gliomas, pose significant challenges due to their complex growth patterns, infiltrative nature, and the variability in brain structure across individuals, which makes accurate diagnosis and monitoring difficult. Deep learning models have been developed to accurately delineate these tumors. However, most of these models were trained on relatively homogenous high-resource datasets, limiting their robustness when deployed in underserved regions. In this study, we performed segmentation-aware offline data augmentation on the BraTS-Africa dataset to increase the data sample size and diversity to enhance generalization. We further constructed an ensemble of three distinct architectures, MedNeXt, SegMamba, and Residual-Encoder U-Net, to leverage their complementary strengths. Our best-performing model, MedNeXt, was trained on 1000 epochs and achieved the highest average lesion-wise dice and normalized surface distance scores of 0.86 and 0.81 respectively. However, the ensemble model trained for 500 epochs produced the most balanced segmentation performance across the tumour subregions. This work demonstrates that a combination of advanced augmentation and model ensembling can improve segmentation accuracy and robustness on diverse and underrepresented datasets. Code available at: https://github.com/SPARK-Academy-2025/SPARK-2025/tree/main/SPARK2025_BraTs_MODELS/SPARK_NeuroAshanti.

Keywords: Brain Tumor Segmentation · Deep Learning · Ensembling · Data augmentation

1 Introduction

Brain tumors, particularly gliomas, represent a significant challenge in neuro-oncology due to their infiltrative nature, histological heterogeneity, and variable prognosis [1]. Gliomas originate from glial cells such as astrocytes and oligodendrocytes and are categorized by the World Health Organization (WHO) into

grades I to IV based on histological and molecular features [2]. While low-grade gliomas (LGGs) tend to grow slowly and are sometimes curable via surgery, high-grade gliomas (HGGs), including glioblastoma multiforme (GBM), are aggressive and associated with poor outcomes. Despite standard-of-care therapies, median survival for GBM patients remains approximately 16 months [3].

These tumors pose additional challenges due to their complex growth patterns and the variability in brain structure across individuals, which makes accurate diagnosis and monitoring difficult. Timely and precise tumor segmentations from magnetic resonance imaging (MRI) scans are important for improving patient outcomes through better treatment planning and response assessment [4].

Manual segmentation of gliomas from multimodal MRI is considered the clinical gold standard. It is however time-consuming, labor-intensive, and prone to inter- and intra-observer variability [5]. To overcome these limitations, deep learning-based approaches have been employed, demonstrating superior performance and efficiency compared to traditional image processing methods [6, 7]. The Brain Tumor Segmentation (BraTS) Challenge has played a pivotal role in benchmarking and advancing automated glioma segmentation since 2012, offering a standardized dataset that includes preprocessed T1-weighted, T1Gd, T2-weighted, and T2-FLAIR sequences, with expert annotations for enhancing tumor (ET), necrotic and non-enhancing tumor core (NCR/NET), and peritumoral edema (ED) [8].

Despite progress, a persistent bottleneck in deploying deep learning models for clinical segmentation remains the limited size and diversity of training datasets. This problem becomes especially pronounced when models are applied to out-of-distribution populations [9]. The recently introduced BraTS-Africa dataset begins to address this gap by providing multimodal MRI scans of glioma patients from healthcare institutions in sub-Saharan Africa. It includes 146 annotated cases, 95 adult diffuse gliomas, and 51 other central nervous system neoplasms reviewed by radiologists certified by the American Board of Radiology [10, 11]. The BraTS-Africa dataset is relatively small, and the variability in scanner quality, clinical settings, and imaging protocols presents further challenges. As a result, training highly accurate and robust segmentation models in these settings remains an open problem, especially under data-limited conditions and diverse real-world constraints.

1.1 Related Works

Over the past decade, convolutional neural networks (CNNs) have emerged as the predominant approach for brain tumor segmentation, particularly in benchmark challenges such as BraTS [8, 12]. Among these, U-Net and its many derivatives have become foundational, since the launch of the BraTS challenge in 2014, due to their encoder-decoder architecture with skip connections, which help preserve spatial information critical for accurate medical image segmentation [13]. To improve performance, these models have been progressively enhanced with architectural innovations such as attention gates, residual connections, and cascaded refinement stages [14, 15]. Over time, top-performing solutions began to

integrate ensemble learning techniques by combining predictions from multiple U-Net variants to reduce model variance and enhance generalization [16, 17].

A major advancement was made with the introduction of nnU-Net. It has been the base model of winning solutions in BraTS 2020 [18], 2021 [19], and 2022 [20]. By 2023, this trend evolved further, with the winning team employing an ensemble of a SwinUNETR and nnU-Net to improve tumor subregion segmentation. Complementary strategies like aggressive augmentation, GAN-generated data, and ensemble-based label refinement have also been used to address class imbalance and reduce overfitting [1]. Modern segmentation models such as MedNeXt [21] have moved beyond the traditional U-net architecture. The model was validated across multiple benchmarks, including BraTS, showing that MedNeXt matches or surpasses nnU-Net in accuracy while maintaining scalability and robustness across diverse tumor types and imaging conditions [21]. Newer approaches such as the State Space based [22] SegMamba have been proposed to address the high computational demands of the Transformer-based models like SwinUNETR.

Our approach builds on recent advances by exploring both model diversity and advanced data augmentation strategies. We ensemble three distinct architectures; MedNeXt, SegMamba, and Residual-Encoder U-Net (ResEnc U-Net), to leverage the complementary strengths of convolutional neural networks and state-space models. To address limited data sample size and variability, we implement a segmentation-aware offline data augmentation pipeline that combines standard geometric and intensity-based transformations together with a custom label-masked elastic deformation to generate diverse and anatomically plausible samples. The label-masked transform applies aggressive elastic deformations specifically to the tumor regions. This targeted augmentation increases variability within the lesion context, thereby enhancing model generalization in data-limited settings such as those represented in the BraTS-Africa dataset.

2 Methods

2.1 Data Description

This study utilized the BraTS-Africa dataset from the MICCAI-CAMERA-Lacuna Fund BraTS-Africa 2025 Challenge, which comprises 95 preoperative glioma cases (60 for training and 35 for validation)[23]. Each case consists of four MRI sequences: T1-weighted (T1), T1-Contrast Enhanced (T1-CE), T2-weighted (T2), and T2-Fluid Attenuated Inversion Recovery (T2-FLAIR). These modalities provide complementary structural and pathological details that are important for accurate tumour assessment and segmentation. The corresponding ground truth labels were manually annotated by expert radiologists and define three tumor subregions, namely the Enhancing Tumour (ET), Non-enhancing Tumour Core (TC), and Whole Tumour (WT). ET represents regions with contrast uptake on post-contrast T1 images, TC includes necrotic or cystic components that lack enhancement, and WT corresponds to peritumoral edema, which is visible on FLAIR sequences.

2.2 Data Expansion

Given the limited sample size of the dataset, segmentation-aware offline data augmentation pipeline was implemented. This approach was adopted to increase the number of data samples, thereby enhancing model generalizability and robustness across varied anatomical presentations of brain tumours, which are important for brain tumour segmentation.

Segmentation-Aware Offline Data Augmentation : This augmentation pipe-line combines affine, flip, bias-field, and elastic deformation transforms from the TorchIO [24] library, and a custom label-mask transform. All the transforms were chained, and predefined probabilities were assigned to all except the label-mask transform, which was applied deterministically. This introduced controlled variation and generation of new samples with realistic brain anatomical characteristics as seen in Figure 1(b).

Complementing the whole brain transformation, the label-mask transform applied rigorous elastic deformation only within the tumour regions of the subject. This preserved the structural integrity of the surrounding brain tissue, enabling targeted morphological changes to the tumour shape and boundary.

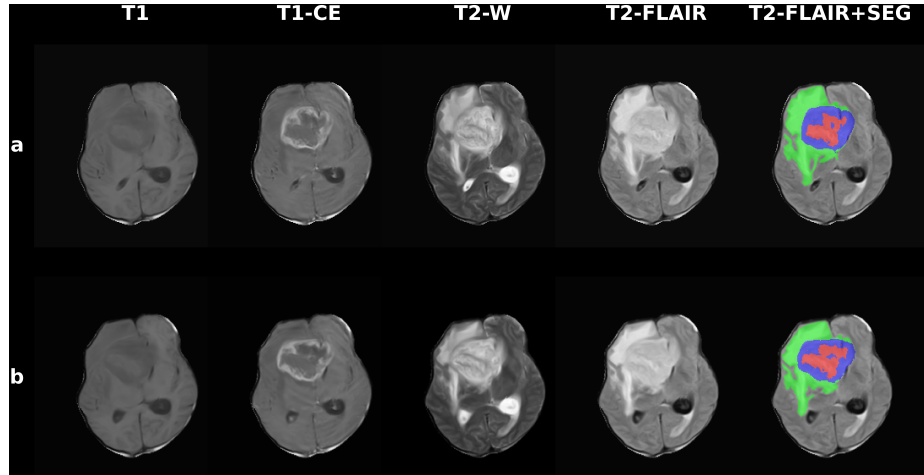


Fig. 1. Axial slices of multi-parametric MRI sequences from the BraTS-Africa dataset. (a) Original sample (BraTS-SSA-00007-000). (b) Augmented version of (a) using segmentation-aware offline data augmentation. Columns show T1, T1CE, T2-W, T2-FLAIR, and T2-FLAIR with segmentation overlay, where the ET, TC and WT are represented in blue, red, and green respectively.

2.3 Models

Multiple segmentation models were selected to explore how variations in their strengths contribute to brain tumour segmentation. All models were trained using the nnU-Net framework to utilize its streamlined pipeline for data pre-processing, training, and inference. Additionally, an ensemble of the selected models was implemented to harness the distinct advantages of each architecture.

SegMamba: SegMamba is a novel 3D medical image segmentation model that incorporates a U-shaped architecture with Mamba, a state space model designed for long-range dependency modelling [25]. Unlike transformer-based approaches, SegMamba can efficiently capture both global and multiscale features from an entire input volumetric space with less computational overhead. The architecture consists of a 3D encoder with multiple Tri-orientated Spatial Mamba (TS-Mamba) blocks for multiscale global feature modelling, a convolution-based decoder, and skip connections with Feature-level Uncertainty Estimation (FUE) modules to refine features from the encoder that are fed to the upsampling path.

MedNeXt: MedNeXt is a fully convolutional segmentation model that employs ConvNeXt blocks in its encoder and decoder, combining the inherent inductive bias of convolutional networks with the scalable design principles of Transformer architectures [21]. The model replaces conventional upsampling and downsampling layers with residual inverted bottlenecks to preserve semantic feature details, leverages an upsampling-based kernel to smoothly transfer pre-trained weights from smaller to larger kernels, and supports compound scaling in depth, width, and kernel size for flexible adaptability across diverse segmentation tasks.

Residual-Encoder U-NET: Residual-Encoder U-Net is a derivative of the original nnU-Net framework that introduces residual connections into the encoder pathway [26]. This architectural network replaces the plain convolutional blocks in the encoder with residual blocks, which reinforce feature representations and gradient flow in deep networks. The decoder structure and overall topology remain consistent with the standard implementation, ensuring compatibility with the self-adapting configuration pipeline of nnU-Net. This modification helps improve learning efficiency and model performance, particularly in deep networks, and it is well-suited for challenging segmentation tasks such as brain tumour segmentation, where detecting subtle variations in tumour appearance is important.

2.4 Experiments

A series of experiments were conducted to evaluate the performance of our selected models on the BraTS-Africa dataset along with the augmented datasets. Each model was initially trained from scratch for 50 epochs using the original

BraTS-Africa dataset. Training continued for 500, and then a 1000 epochs using the best saved model weights checkpoint to assess the impact of extended training durations on segmentation performance. All models were trained in a 5-fold cross validation manner, using a composite loss function of Dice and Cross-Entropy loss to balance region-level and voxel-wise accuracy. Stochastic Gradient Descent (SGD) was employed as the optimizer, with a cosine annealing learning rate schedule initialized at 1e-4.

In creating the offline augmented dataset, transformations were applied 5 times per sample to the training set, forming a total of 300 cases.

Segmentation performance was evaluated using standard metrics, including Lesion-Wise Dice (LSD) and Normalized Surface Distance (NSD) at 1.00 mm for the Enhancing Tumor (ET), Non-enhancing Tumor Core (TC), and Whole Tumor (WT) subregions. Model predictions on the 35 validation cases were submitted to the synapse platform for evaluation.

3 Results

3.1 Segmentation Performance

Tables 1 and 2 summarize the segmentation performance of SegMamba, MedNeXt, Residual-Encoder U-Net, and the ensemble across different training configurations.

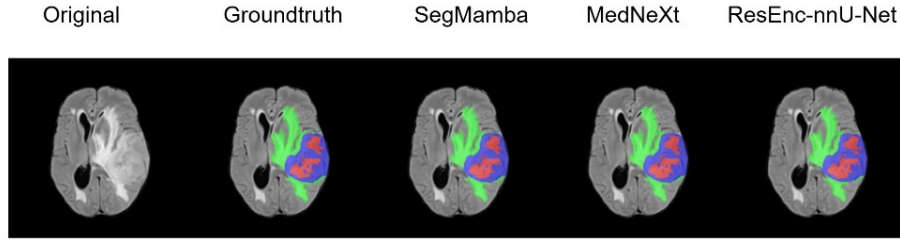


Fig. 2. Predictions of the three tumour subregions (TC in red, ET in blue, WT in green) by each of the models. Order of images: Original, Ground truth, SegMamba, MedNeXt, ResEnc U-Net, from sample BraTS-SSA-00141-000.

4 Discussion and Conclusion

This study investigated the segmentation performance of three distinct deep learning models, MedNeXt, SegMamba, and ResEnc U-Net and their ensemble, on the BraTS-Africa dataset under varying training setups. The findings reveal

Table 1. Results of the experiments comparing individual model performance (LSD - Lesion-Wise Dice and NSD_1.0 mm - Normalized Surface Distance at 1.00 mm) across the tumor subregions Enhancing Tumor (ET), Tumor Core (TC), and Whole Tumor (WT), as well as their overall average (AVG), under different training durations and settings. Each method is denoted by its initial: S for SegMamba, M for MedNeXt, and R for ResEnc U-Net, followed by the corresponding training configuration. Best results per column are in **Bold**.

Method	LSD				NSD 1.0 mm			
	ET	TC	WT	AVG	ET	TC	WT	AVG
S_{50e}	0.796	0.790	0.877	0.821	0.786	0.714	0.777	0.759
M_{50e}	0.799	0.794	0.879	0.824	0.793	0.729	0.790	0.771
R_{50e}	0.791	0.787	0.881	0.820	0.777	0.704	0.783	0.755
S^{aug}_{50e}	0.799	0.785	0.871	0.818	0.761	0.770	0.699	0.743
M^{aug}_{50e}	0.804	0.790	0.887	0.827	0.782	0.715	0.776	0.758
R^{aug}_{50e}	0.791	0.783	0.857	0.810	0.835	0.770	0.823	0.809
S_{500e}	0.806	0.790	0.892	0.829	0.795	0.717	0.797	0.770
M_{500e}	0.836	0.831	0.912	0.860	0.789	0.725	0.778	0.764
R_{500e}	0.801	0.798	0.866	0.822	0.789	0.725	0.778	0.764
S_{1000e}	0.801	0.781	0.893	0.825	0.792	0.715	0.801	0.769
M_{1000e}	0.855	0.844	0.896	0.865	0.846	0.775	0.808	0.810
R_{1000e}	0.800	0.796	0.864	0.820	0.790	0.726	0.778	0.765
M^{aug}_{1000e}	0.836	0.838	0.876	0.850	0.831	0.775	0.775	0.794

Table 2. Results of the ensemble experiments (LSD - Lesion-Wise Dice and NSD_1.0 mm - Normalized Surface Distance at 1.00 mm) across the tumor subregions Enhancing Tumor (ET), Tumor Core (TC), and Whole Tumor (WT), as well as their overall average (AVG). Ensembles are denoted by listing their constituent models: S (SegMamba), M (MedNeXt), and R (ResEnc U-Net). Best results are in **Bold**.

Ensemble Method	LSD				NSD 1.0 mm			
	ET	TC	WT	AVG	ET	TC	WT	AVG
$S+M+R_{50e}$	0.795	0.787	0.881	0.821	0.787	0.717	0.791	0.765
$S+M+R_{500e}$	0.846	0.843	0.896	0.861	0.839	0.775	0.812	0.809
$S+M+R_{1000e}$	0.857	0.842	0.883	0.861	0.847	0.772	0.798	0.806
$S+M_{1000e}$	0.824	0.810	0.895	0.843	0.814	0.740	0.806	0.787
$M+R_{1000e}$	0.860	0.846	0.897	0.867	0.852	0.780	0.812	0.815
$M+R+M^{\text{aug}}_{1000e}$	0.848	0.843	0.898	0.863	0.843	0.780	0.816	0.813

that the model architecture, augmentation approach, training configuration and integration strategy play a significant role in determining segmentation accuracy, particularly within data-limited and anatomically diverse cases.

Training duration had a notable impact on model performance. Across all architectures, extending training epochs generally led to improved segmentation results. This trend was apparent in the MedNeXt model, which recorded the highest average LSD of **0.865** and NSD of **0.810** at 1000 epochs (M_{1000e}). Interestingly, the best WT segmentation performance in terms of LSD, with a score of **0.912**, was achieved by the MedNeXt-model trained for 500 epochs (M_{500e}). This suggests that optimal performance on individual tumour subregions may not always correlate linearly with increased training duration. In contrast, SegMamba showed diminishing results beyond 500 epochs, suggesting that optimal training duration may vary depending on architectural characteristics and convergence behavior.

MedNeXt consistently outperformed the other models across both LSD and NSD metrics, likely due to its ability to preserve spatial information through its ConvNeXt residual blocks and efficient scaling. SegMamba demonstrated competitive performance as well, particularly for WT segmentation. This may be due to its state-space modelling and better global context encoding capabilities. The ResEnc U-Net showed stable but slightly lower performance, which may be attributed to its relatively simpler architectural design.

The segmentation-aware augmented dataset yielded NSD improvements for some models compared to their baselines. The R^{aug}_{50e} recorded NSD scores of **0.835**, **0.770**, and **0.823** for ET, TC, and WT respectively, with its WT score being the highest among all models and its average NSD increasing from **0.755** to **0.809**. S^{aug}_{50e} showed a notable increase in TC NSD, although its overall average NSD declined slightly. Meanwhile, M^{aug}_{50e} exhibited a small decrease in average NSD, suggesting that augmentation may not consistently benefit all architectures. While its effects varied across models, the observed improvements highlight the benefit of targeted augmentation in improving boundary-level segmentation performance.

The ensemble models consistently outperformed their individual counterparts in both LSD and NSD metrics, confirming the benefit of combining diverse architectural representations. The $M+R_{1000e}$ configuration achieved the highest average NSD of **0.815** and tied for the highest LSD of **0.867**. The Residual-Encoder U-Net was initially excluded from the ensemble (results indicated by $S+M_{1000e}$) based on the assumption that its standalone performance was inferior to the other models. However, its inclusion was later shown to enhance overall ensemble performance, suggesting that it contributed meaningfully to the final predictions. Another noteworthy observation was that, although SegMamba achieved competitive standalone performance, its removal from the ensemble unexpectedly led to a slight improvement in overall results. This outcome suggests that not all high-performing models contribute positively when combined, and that ensemble behavior may depend on how different architectures how they interpret MRI modalities differently, as shown by Ren et al. [27]. Future work

should examine how these differences affect ensemble performance. Collectively, these findings suggest that integrating multiple architectures produces a more balanced and generalizable model and highlights its potential for use in clinical contexts where these attributes are essential.

Although increasing training duration generally improved model performance, the variation in fold usage and training epochs from 50 to 1000 may have led to unstable learning in certain configurations. A more uniform strategy, such as training all models on the same folds and applying a cosine annealing schedule with warm restarts, could have yielded smoother convergence and better generalization. Future work can explore such dynamic scheduling approaches to stabilize training across folds and enhance performance without significantly increasing runtime.

Overall, the findings demonstrate that brain tumour segmentation performance is influenced by the type of model architecture, training configuration, augmentation strategy, and ensemble learning. Leveraging these factors collectively in this study supports the development of robust brain tumour segmentation models with improved generalizability, suitable for deployment in Sub-Saharan Africa and other resource-limited medical imaging settings.

Acknowledgments. The authors would like to thank the following instructors of the Sprint AI Training for African Medical Imaging Knowledge Translation (SPARK) Academy 2025 summer school on deep learning in medical imaging for providing insightful background knowledge on brain tumours that informed the research presented here; Noha Magdy, Maruf Adewole, Ayomidale B. Oladele, Amal Saleh, Nourou Dine Bankole, Jeremiah Fadugba, Lorumbur Moses, Toufiq Musah, Teresa Zhu, Craig Jones, Confidence Raymond, Lukman E. Ismaila, Ugumba Kikwima, Mehdi Astaraki, Peter Hastreiter, Evan Calabrese, Esin Uzturk Isik, Navodini Wijethilake, Rancy Chepchirchir, James Gee, MacLean Nasrallah, Jean Baptiste Poline, Bijay Adhikari, Kenneth Agu, Mohannad Barakat & Yahoo Liu. The authors would also like to thank Linshan Liu for administrative assistance in supporting the SPARK Academy training and capacity-building activities, which the authors immensely benefited from. The authors acknowledge the computational infrastructure support from the Digital Research Alliance of Canada (The Alliance) and the University of Washington Azure GenAI for Science Hub through The eScience Institute and Microsoft (PI: Mehmet Kurt) secured for the SPARK Academy. Finally, we would like to thank the Lacuna Fund for Health and Equity, the Radiological Society of North America (RSNA), the Research & Education (R&E) Foundation Derek Harwood-Nash International Education Scholar Grant, the McGill University Healthy Brain and Healthy Lives (HBHL) and the National Science and Engineering Research Council of Canada (NSERC) Discovery Launch Supplement for making the SPARK Academy possible via research grant supports.

Disclosure of Interests. The authors have no competing interests to declare that are relevant to the content of this article

References

- [1] André Ferreira et al. “How we won brats 2023 adult glioma challenge? just faking it! enhanced synthetic data augmentation and model ensemble for brain tumour segmentation”. In: *arXiv preprint arXiv:2402.17317* (2024).
- [2] Usharani Bhimavarapu, Nalini Chintalapudi, and Gopi Battineni. “Brain tumor detection and categorization with segmentation of improved unsupervised clustering approach and machine learning classifier”. In: *Bioengineering* 11.3 (2024), p. 266.
- [3] David N Louis et al. “The 2016 World Health Organization classification of tumors of the central nervous system: a summary”. In: *Acta neuropathologica* 131.6 (2016), pp. 803–820.
- [4] KS Neetha and Dayanand Lal Narayan. “Segmentation and classification of brain tumour using LRIFCM and LSTM”. In: *Multimedia Tools and Applications* 83.31 (2024), pp. 76705–76730.
- [5] Brent Foster et al. “A review on segmentation of positron emission tomography images”. In: *Computers in biology and medicine* 50 (2014), pp. 76–96.
- [6] Sheng-Yao Huang et al. “Fully convolutional network for the semantic segmentation of medical images: A survey”. In: *Diagnostics* 12.11 (2022), p. 2765.
- [7] Konstantinos Kamnitsas et al. “Efficient multi-scale 3D CNN with fully connected CRF for accurate brain lesion segmentation”. In: *Medical image analysis* 36 (2017), pp. 61–78.
- [8] Bjoern H Menze et al. “The multimodal brain tumor image segmentation benchmark (BRATS)”. In: *IEEE transactions on medical imaging* 34.10 (2014), pp. 1993–2024.
- [9] Christopher J Kelly et al. “Key challenges for delivering clinical impact with artificial intelligence”. In: *BMC medicine* 17.1 (2019), p. 195.
- [10] Sverre Helge Torp, Ole Solheim, and Anne Jarstein Skjulsvik. “The WHO 2021 Classification of Central Nervous System tumours: a practical update on what neurosurgeons need to know—a minireview”. In: *Acta neurochirurgica* 164.9 (2022), pp. 2453–2464.
- [11] Maruf Adewole et al. “The BraTS-Africa Dataset: Expanding the Brain Tumor Segmentation Data to Capture African Populations”. In: *Radiology: Artificial Intelligence* 7.4 (2025), e240528.
- [12] Spyridon Bakas et al. “Identifying the best machine learning algorithms for brain tumor segmentation, progression assessment, and overall survival prediction in the BRATS challenge”. In: *arXiv preprint arXiv:1811.02629* (2018).
- [13] Olaf Ronneberger, Philipp Fischer, and Thomas Brox. “U-net: Convolutional networks for biomedical image segmentation”. In: *International Conference on Medical image computing and computer-assisted intervention*. Springer. 2015, pp. 234–241.
- [14] Ozan Oktay et al. “Attention u-net: Learning where to look for the pancreas”. In: *arXiv preprint arXiv:1804.03999* (2018).

- [15] Zan Li et al. “Residual-attention UNet++: a nested residual-attention U-net for medical image segmentation”. In: *Applied Sciences* 12.14 (2022), p. 7149.
- [16] Fabian Isensee et al. “nnU-Net: a self-configuring method for deep learning-based biomedical image segmentation”. In: *Nature methods* 18.2 (2021), pp. 203–211.
- [17] Andriy Myronenko. “3D MRI brain tumor segmentation using autoencoder regularization”. In: *International MICCAI brainlesion workshop*. Springer. 2018, pp. 311–320.
- [18] Fabian Isensee et al. “nnU-Net for brain tumor segmentation”. In: *International MICCAI Brainlesion Workshop*. Springer. 2020, pp. 118–132.
- [19] Huan Minh Luu and Sung-Hong Park. “Extending nn-UNet for brain tumor segmentation”. In: *International MICCAI brainlesion workshop*. Springer. 2021, pp. 173–186.
- [20] Ramy A Zeineldin et al. “Multimodal CNN networks for brain tumor segmentation in MRI: a BraTS 2022 challenge solution”. In: *International MICCAI Brainlesion Workshop*. Springer. 2022, pp. 127–137.
- [21] Saikat Roy et al. “Mednext: transformer-driven scaling of convnets for medical image segmentation”. In: *International Conference on Medical Image Computing and Computer-Assisted Intervention*. Springer. 2023, pp. 405–415.
- [22] Albert Gu and Tri Dao. “Mamba: Linear-time sequence modeling with selective state spaces”. In: *arXiv preprint arXiv:2312.00752* (2023).
- [23] Maruf Adewole et al. “The brain tumor segmentation (brats) challenge 2023: Glioma segmentation in sub-saharan africa patient population (brats-africa)”. In: *ArXiv* (2023), arXiv–2305.
- [24] Fernando Pérez-García, Rachel Sparks, and Sébastien Ourselin. “TorchIO: a Python library for efficient loading, preprocessing, augmentation and patch-based sampling of medical images in deep learning”. In: *Computer methods and programs in biomedicine* 208 (2021), p. 106236.
- [25] Zhaohu Xing et al. “Segmamba: Long-range sequential modeling mamba for 3d medical image segmentation”. In: *International conference on medical image computing and computer-assisted intervention*. Springer. 2024, pp. 578–588.
- [26] Kaiyuan Ji et al. “Application of 3D nnU-Net with residual encoder in the 2024 MICCAI head and neck tumor segmentation challenge”. In: *Challenge on Head and Neck Tumor Segmentation for MRI-Guided Applications*. Springer, 2024, pp. 250–258.
- [27] Tianyi Ren et al. “Here Comes the Explanation: A Shapley Perspective on Multi-contrast Medical Image Segmentation”. In: *arXiv preprint arXiv:2504.04645* (2025).